Macromolecules

ARTICLE

pubs.acs.org/Macromolecules

Cross-Linking of Side Chain Unsaturated Aromatic Polyethers for High Temperature Polymer Electrolyte Membrane Fuel Cell Applications

Konstantinia D. Papadimitriou,[†] Fotis Paloukis,[§] Stylianos G. Neophytides,[‡,§] and Joannis K. Kallitsis[†,‡,§,*]

[†]Department of Chemistry, University of Patras, Patras 26500, Greece

[‡]Foundation of Research and Technology-Hellas, Institute of Chemical Engineering and High Temperature Processes (FORTH-ICE/HT), Patras 26504, Greece

[§]Advent Technologies S.A., Patras Science Park, Stadiou Str., Patras 26504, Greece

ABSTRACT: Novel aromatic polyethers bearing polar pyridine units along the main chain and side cross-linkable propenyl groups have been successfully synthesized. Their properties relating to their ability to be used as polymer electrolyte membranes for high temperature fuel cell applications, were thoroughly investigated. Cross-linked membranes were obtained by thermal curing of the cross-linkable polymers with the use of a bisazide as the cross-linking agent. The glass transition temperatures of the cross-linked membranes were determined by dynamic mechanical analysis and found to be higher compared to the neat polymers proving the successful cross-linked network. The doping ability in phosphoric acid and the proton conductivity of the cross-linked membranes were higher compared to the noncross-linked analogues. Finally, membrane electrode assemblies (MEAs) were constructed and tested in a single cell at temperatures between 180 and 220 °C. The superior performance of the cross-linked membranes in combination with the operating stability at 200 °C for 48 h demonstrate the potential use of these materials as electrolytes for high temperature PEM fuel cells.

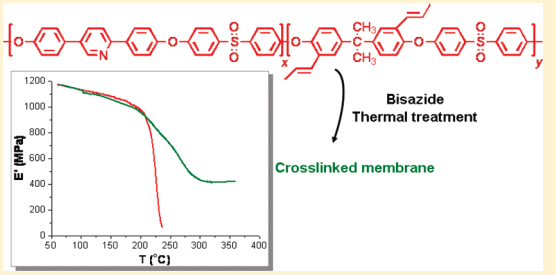

1. INTRODUCTION

Over the last few decades a continuously growing scientific interest is observed for polymer electrolyte membranes for fuel cell applications (PEMFCs).[1,2] This is due to the fact that this technology can be a key factor in the development of environmentally friendly economies, since it can be used for energy supply in transport, stationary and mobile applications. The proton exchange membrane (PEM) is the core of a fuel cell device, which must combine a lot of prerequisities such as high ionic conductivity, high thermal, mechanical and chemical stability, and low fuel or gas permeability as well as low cost. The most commonly used proton exchange membrane for fuel cells operating at temperatures below 100 °C are perfluorinated ionomers such as Nafion produced by DuPont. Although these polymers fulfill the main requirements, their low conductivity at low humidity or high temperatures as well as their high methanol diffusion in the case of the direct methanol fuel cells (DMFCs) have limited their application.[3−7]

The above-mentioned drawbacks in combination with the high cost of these materials turned the scientific research in the development of different polymeric membranes. In this category, sulfonated aromatic polyethers have been studied as alternatives to Nafion due to their good physical properties and high ionic conductivities.[3,8−13] For these polymers, a high degree of sulfonation is required in order to reach high water uptakes and thus to achieve the desired ionic conductivity. However, such a high sulfonation level results in significant swelling in water and high methanol diffusion which leads to the loss of the mechanical properties of the membranes.[14,15]

One effective approach to reduce water swelling and to enhance the mechanical stability of the membranes is the cross-linking method, which includes the ionic and covalent cross-linking. Ionic cross-linking is based on interaction forces between different types of ionomers such as acid−base polymers and results in PEMs not only with low water uptake and methanol diffusion but also improved stability and mechanical strength.[16−23] Nevertheless, ionic cross-linking is not effective at high temperatures where the membranes lose their mechanical properties. On the other hand, covalently cross-linked systems preserve the characteristics of the cross-linked membranes even at elevated temperatures which is desirable for many reasons.[24,25]

PEMFC technology operating at temperatures above 100 °C improves the CO tolerance of the Pt electrodes, provides higher energy efficiency and simplifies heat management. The most studied polymer electrolyte for use in high temperature fuel cells, is polybenzimidazole (PBI) doped with phosphoric acid due to its high ionic conductivity and excellent thermal stability.[26−29] Alternative and promising polymers for the same use are the aromatic polyethers bearing polar groups in the main polymeric backbone.[30−33] Our group reported the synthesis of aromatic polyethers containing polar pyridine units and phosphine oxide

Received: February 15, 2011
Revised: April 18, 2011
Published: May 18, 2011

dx.doi.org/10.1021/ma200351z | *Macromolecules* 2011, 44, 4942–4951

or sulfone moieties in the main chain which shown promising results for applications in PEMFCs. These polymers besides their low cost, possess high thermal, mechanical and oxidative stability. Furthermore, the polar groups interact with the phosphoric acid to obtain the desired ionic conductivity.[32,33]

Nevertheless, a crucial problem of all the aforementioned polymer electrolytes is the deficient long-term durability of these systems at temperatures as high as 200 °C. Hence, the challenge to find materials that show even greater mechanical stability with adequate ionic conductivities still remains. A promising approach to overcome this problem is the covalent cross-linking. To this direction many efforts have been made to cross-link sulfonated aromatic polyethers containing reactive double bonds either by UV irradiation using appropriate initiators or by thermal treatment with the use of cross-linking agents.[34−41] In addition, the chemical cross-linking of sulfonated poly(arylene ether)s containing ethynyl groups has been reported.[42−45]

However, all the above reports are focused on sulfonated polyelectrolytes for use in low temperature PEM fuel cells. In this report we explore the possibility to create cross-linked polymers with the aim of achieving membranes able to be used at higher operating temperatures. So, we present the synthesis of aromatic polyethers containing polar pyridine units in the main chain and side cross-linkable propenyl groups. These polymers were subjected to thermal cross-linking with the use of a bisazide as the cross-linker. In this respect we try to improve the mechanical properties in terms of glass transition temperature as well as the stability of the doped membranes by hindering the rupture of the membrane-electrode assemblies (MEAs) under operating conditions. The effect of the cross-linking on the thermal and mechanical properties and on the phosphoric acid doping ability of the membranes was studied. Selected cross-linked membranes were tested in single cells operating at high temperatures, even up to 220 °C.

2. EXPERIMENTAL SECTION

2.1. Materials. 2,5-Bis(4-hydroxyphenyl)pyridine[30] and bis(4-fluorophenyl)phenylphosphine oxide[46] were prepared according to literature procedures. All other chemicals and solvents were purchased from Aldrich and Merck and were used without further purification.

2.2. Instrumentation. ^{1}H NMR spectra were obtained on a Bruker Advance DPX spectrometer at 400 MHz. The samples were dissolved in deuterated chloroform with TMS as internal standard. Size exclusion chromatography (SEC) measurements were carried out using a Polymer Lab chromatographer equipped with two Plgel 5 μm mixed columns and a UV detector (254 nm), using $CHCl_3$ as eluent with a flow rate of 1 mL/min at 25 °C and polystyrene standards in the 1000−500 000 MW range. Thermogravimetric analysis (TGA) was carried out on 10 mg samples contained in alumina crucibles in a Labsys TG of Setaram under nitrogen and at a heating rate of 10 °C/min. DMA measurements were performed using a solid state analyzer RSA II, Rheometrics Scientific Ltd., at 10 Hz. Conductivity measurements were carried out by the current interruption method using a potentiostat/galvanostat (EG and G model 273) and an oscillator (Hitachi model V-650F). FTIR spectra were recorded on a Perkin-Elmer 16PC FTIR spectrometer.

2.3. Synthesis of Copolymers P[Py(*x*)-Pro(*y*)/SO_2]. To a degassed flask equipped with a Dean−Stark trap were added a mixture of bis(4-fluorophenyl) sulfone (1.000 g, 3.93 mmol), 2,5-bis(4-hydroxyphenyl)pyridine (0.8272 g, 3.14 mmol), 2,2′-diallyl bisphenol A (0.2426 g, 0.78 mmol), K_2CO_3 (0.6269 g, 4.56 mmol), toluene (5.0 mL), and DMSO (15.0 mL). The mixture was degassed under argon and stirred at 140 °C for 16 h. After distilling off the azeotropic mixture of the formed water with toluene, the temperature was gradually raised at 180 °C for 6 h. The viscous solution was poured into methanol to precipitate out the polymer, filtered off, stirred in water at 60 °C, and dried at 80 °C under vacuum for 24 h. The results are summarized in Table 1.

Table 1. Characteristics of the Cross-Linkable Polymers

polymer	x/y^a	$M_n{}^b$	M_w	M_w/M_n
	Copolymers P[Py(*x*)-Pro(*y*)/SO_2]			
Ia	60/40	22 000	46 110	2.0
Ib	70/30	33 830	92 100	2.7
Ic	70/30	17 240	33 200	1.9
Id	75/25	41 850	113 390	2.7
Ie	80/20	64 870	155 890	2.4
	Copolymers P[Py(*x*)-Pro(*y*)/PO]			
IIa	64/36	14 000	27 500	1.9
IIb	70/30	15 600	31 000	1.9
IIc	80/20	31 230	50 180	1.6
IId	80/20	14 000	23 700	1.7
	Homolymer P[Pro(100)/SO_2]			
III	-	41 870	110 330	2.6

[a] Compositions as determined by the ^{1}H NMR characterization. [b] GPC in $CHCl_3$ and calibration using PS standards.

2.4. Synthesis of Copolymers P[Py(*x*)-Pro(*y*)/PO]. The same procedure was followed for the synthesis of copolymers P[Py(*x*)-Pro(*y*)/PO] using bis(4-fluorophenyl)phenylphosphine oxide as the difluoride reagent instead of bis(4-fluorophenyl) sulfone. (Scheme 1). A mixture of bis(4-fluorophenyl)phenylphosphine oxide (1.000 g, 3.18 mmol), 2,5-bis(4-hydroxy-phenyl) pyridine (0.6698 g, 2.54 mmol), 2,2′-diallyl bisphenol A (0.1964 g, 0.63 mmol), K_2CO_3 (0.5098 g, 3.69 mmol), toluene (5.0 mL) and DMSO (15.0 mL) was stirred at 140 °C for 16 h and at 180 °C for 8 h. The viscous solution was precipitated in methanol, filtered off, stirred in water at 60 °C, and dried at 80 °C under vacuum for 24 h. The results are summarized in Table 1.

2.5. Fabrication of the Cross-Linked Membranes. The dried polymers were dissolved in dimethylacetamide (DMAc) at a 3 wt % concentration, at room temperature. In this solution different amounts of the commercially available bisazide 2,6-bis(4-azidobenzylidene)-4-methylcyclohexanone, which was used as the cross-linking agent, were added as seen in Table 2. The chemical structures of the cross-linked membranes are represented in Scheme 2. The mixture was then filtered and the membranes were obtained using the solution-casting method where the solvent was left to evaporate at 140 °C for 24 h and then the temperature was elevated at 200 °C for 5 more hours to complete the cross-linking procedure. The obtained films were then dried under vacuum at 160 °C for 3 days. For comparison, membranes of the neat polymers were fabricated in the same method without the addition of the cross-linking agent.

2.6. Doping Procedures. The impregnated membranes were obtained by immersing samples into 85% phosphoric acid solution at a certain temperature for different doping times. After each immersion the samples were wiped with paper and the weight gain was calculated from the samples' weight before and after the immersion. The doping level is defined as the weight percent of the phosphoric acid per gram of each membrane. Temperature and doping time varied, for each polymer sample to reach the maximum doping level.

2.7. Treatment with H_2O_2 (Fenton's Test). To perform a test of the oxidative stability of the produced materials, strips of the undoped membranes were immersed into 3% H_2O_2 aqueous solution containing 4 ppm $FeCl_2$ at 80 °C for 72 h. The thickness of the membranes was in

Scheme 1. Synthesis of the Cross-Linkable Copolymers

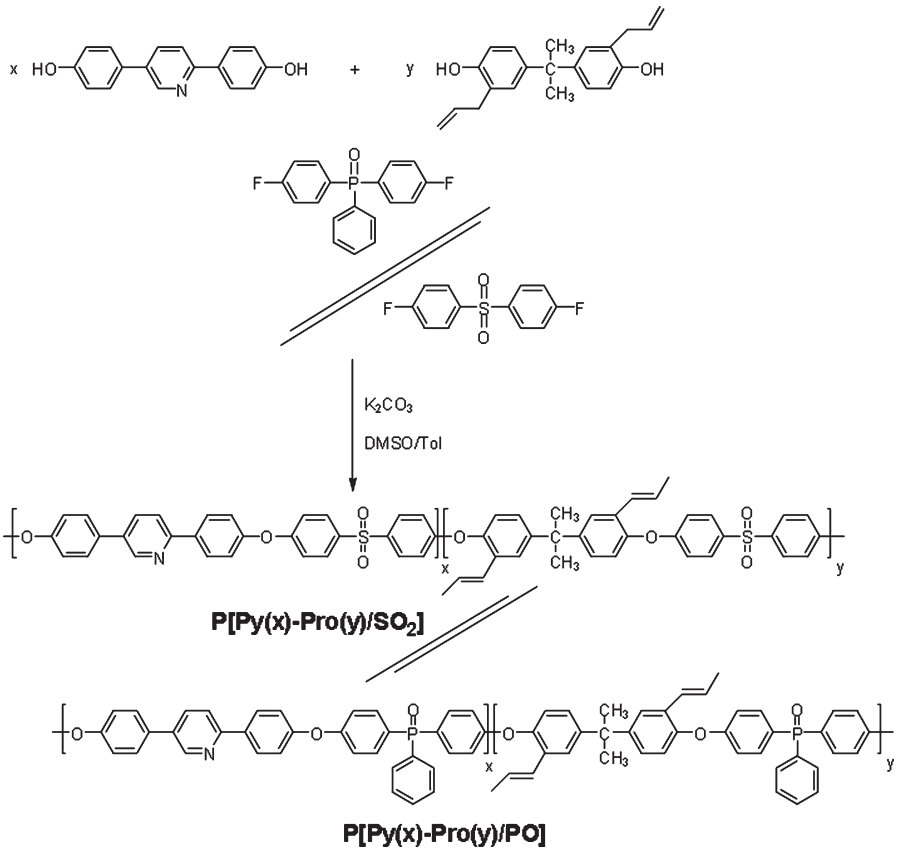

Table 2. Compositions of the Cross-Linked Membranes, T_g Values for the Virgin Polymers and the Cross-Linked Ones and Soluble Percentage of the Cross-Linked Membranes in DMAc

cross-linked polymer	un-cross-linked polymer (wt %)	bisazide (wt %)	T_g[a]	T_g[c]	soluble ercentage[b] (wt %)
		Copolymers P[Py(*x*)-Pro(*y*)/SO_2]			
Ia^{CL}	75	25	198	228	18
Ib^{CL}	70	30	228	290	1
Ic^{CL}	70	30	220	300	5
Id^{CL}	75	25	230	290	5
Ie^{CL}	75	25	230	232	2
		Copolymers P[Py(*x*)-Pro(*y*)/PO]			
IIb^{CL}	70	30	220	242	9
IIc^{CL}	78	22	243	250	24
		Homolymer P[Pro(100)/SO2]			
III^{CL}	40	60	230	-	0

[a] Glass transition temperatures for the virgin polymers obtained by DMA. [b] Soluble percentage in DMAc for the cross-linked membranes after heating at 60 °C for 6 h. [c] Glass transition temperatures for the cross-linked polymers obtained by DMA.

the range of 100−120 μm. After the treatment, the samples were dried under vacuum at 80 °C, and possible changes in thermal and mechanical properties were examined with thermogravimetric analysis (TGA) and dynamic mechanical analysis (DMA).

2.8. Electrodes Preparation and MEA Fabrication. The handmade electrodes were prepared from ink by mixing the catalyst powder (30 wt % Pt/C) and isopropanol as solvent, on a gas diffusion layer (GDL). GDL was homemade using carbon cloth on which was sprayed slurry made of Vulcan carbon and PTFE dispersion (weight ratio PTFE/carbon = 0.3/0.7), followed by sintering at 300 °C under static air for 60 min. Finally, the electrodes were treated for 2 h at 80 °C and 1 h at 120 °C under Ar in order to remove the organic solvent. MEAs were fabricated by placing the electrodes on both sides of the phosphoric acid doped membrane and then hot pressing at 150 °C for 15 min. In this work, the cathode side and the anode side use the same electrodes with catalyst loading ~1.5 mg/cm^2, while the assembling force for the single cell was 4 N m or 0.1 t/cm^2.

2.9. Electrochemical Characterization. The electrochemical evaluation of the MEAs was carried out in a single cell with serpentine flow channels (Fuel Cell Technologies Inc.). The active area of the MEAs was 25 cm^2. Pure hydrogen and air gases were supplied to the anode and cathode compartments, respectively. A constant reactant utilization of 50% for oxygen and 83% for hydrogen were used. All measurements were performed at ambient pressure. Polarization curves were recorded at different temperatures using the potentiostat/galvanostat PGSTAT30. The electrochemical impedance spectra (EIS) were recorded at 0.2 A/cm^2 in the frequency range of 10 mHz to 50 kHz with an amplitude of sinusoidal signal of 50 mA rms, using the same equipment. All measurements reported in this work were made in two-electrode arrangement, with the anode serving as both counter and reference electrode and the cathode used as working electrode.

Scheme 2. Schematic Representation of the Chemical Structures of the Cross-Linked Polymers Using a Bisazide as a Cross-Linker

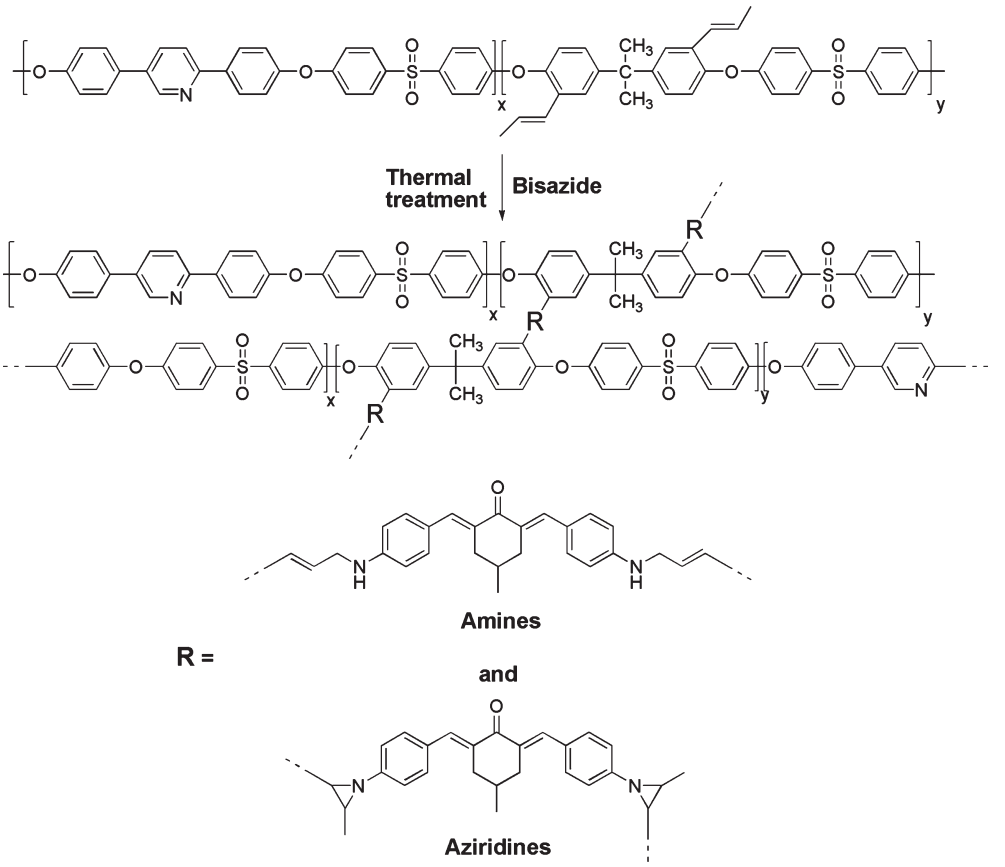

3. RESULTS AND DISCUSSION

As previously reported,[31−33] the aromatic polyethers containing the pyridine and sulfone units in the main chain are promising candidates for use in high temperature fuel cell applications since these materials fulfill the required properties. In this work, in order to further improve the mechanical properties of these polymers and thus to enhance the long-term durability of the MEAs at high temperatures up to 200 °C, we attempted to synthesize cross-linkable aromatic polyethers bearing side propenyl groups via nucleophilic aromatic substitution reactions (Scheme 1). The resulting polymers were all soluble in polar organic solvents, such as $CHCl_3$, DMSO, NMP, and DMA. High molecular weights were obtained in all cases as proven by size exclusion chromatography characterization and are depicted in Table 1. A representative ^{1}H NMR spectrum for polymer **Ia** is given in Figure 1. The peaks between 6.2 and 6.5 ppm are characteristics of the rearrangement of the allyl groups of 2,2′-diallyl bisphenol A into propenyl groups. This is due to the fact that the potassium carbonate under the polymerization conditions acts as a base-catalysis of isomerization of allyl groups to propenyl groups.[47,48] The percentage of the double bonds in the polymeric chain was calculated from the integration ratio of peak a at 8.9 ppm which is assigned to the aromatic proton neighboring the nitrogen in the pyridine ring and peaks c and d of the propenyl groups. These experimental values are in accordance with the theoretical ones calculated from the monomers' feed ratio.

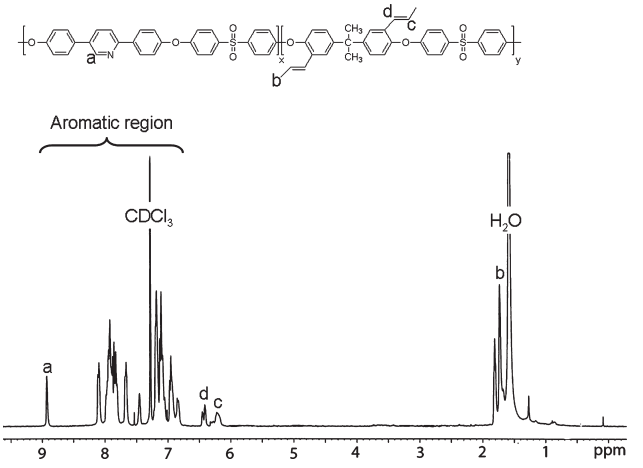

Figure 1. ^{1}H NMR spectrum of the cross-linkable copolymer **Ia**.

The film forming ability of the synthesized polymers allowed the characterization of their thermomechanical properties by means of dynamic mechanical analysis (DMA). In Figure 2 the DMA curves of the **Ia** and **IIb**, **IIc** copolymers, are presented, and in all cases, high T_g values, above 200 °C, were obtained. The glass transition temperatures depend on the bisphenylpyridine copolymers' content, and are reduced at higher percentages of the propenyl moieties. This is due to the increased volume fraction possessed by the side propenyl groups in combination with their higher flexibility.

dx.doi.org/10.1021/ma200351z |*Macromolecules* 2011, 44, 4942–4951

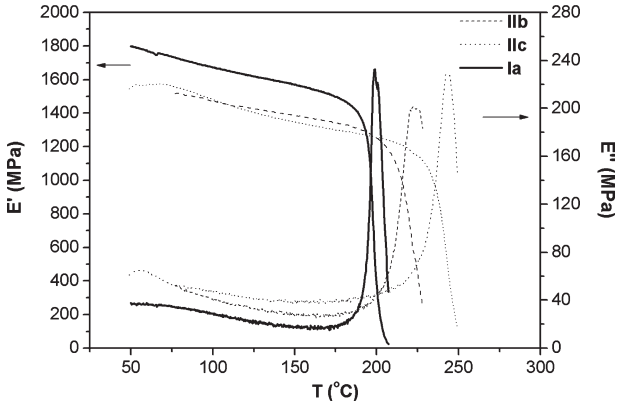

Figure 2. DMA curves of the **Ia** and **IIb**, **IIc** copolymers.

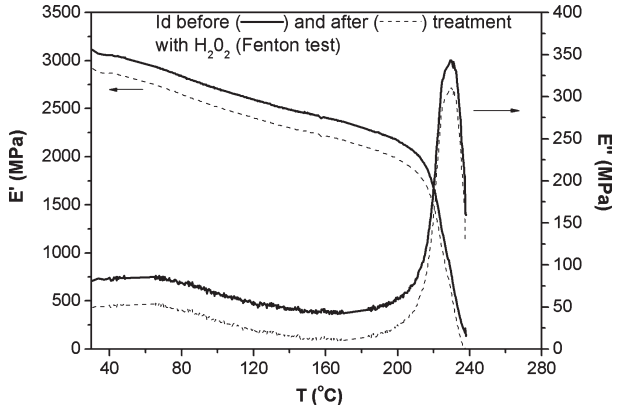

Figure 3. DMA curves of the copolymer **Id** before and after treatment with H_2O_2 (Fenton test).

Fenton test treatment was performed in order to evaluate whether the membranes are able to withstand a strong oxidizing environment during the fuel cell operation.[49,50] Therefore, the membranes produced by different copolymers were treated with 3 wt % H_2O_2 solution in the presence of ferrous ions (4 ppm of $FeCl_2$) for 72 h at 80 °C. The oxidative stability of these copolymers after treatment with the Fenton reagent, was examined with dynamic mechanical analysis and thermogravimetric analysis. As shown, for example in Figure 3, for the copolymer **Ic**, no significant changes occurred after treatment with hydrogen peroxide either to the membrane's integrity or to its mechanical properties compared to the polymer before such a treatment. Moreover, as can be easily seen in Figure 4, the thermal stability of the treated membrane shows a further improvement, probably due to the cross-linking reactions that can happen during the Fenton test treatment. This is mostly evident from the higher residual at temperatures higher than 550 °C which is almost 50 wt % for the treated membrane.

For the use of these materials in high temperature fuel cells, an important prerequisite is their ability to be doped in strong acids thus resulting in high ionically conductive materials. Therefore, the membranes were doped in phosphoric acid 85% at various temperatures. As it can be seen in Figure 5, higher contents in pyridine units increase the doping level of the P[Py(x)-PrO(y)/SO_2] copolymers since these are the only moieties in the polymeric chain which can interact with the phosphoric acid. The copolymers with the phosphinoxide units (Figure 6) absorb

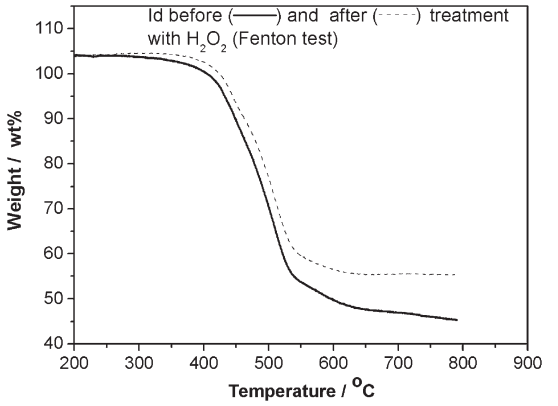

Figure 4. Thermogravimetric analysis of the copolymer **Id** before and after treatment with H_2O_2 (Fenton test).

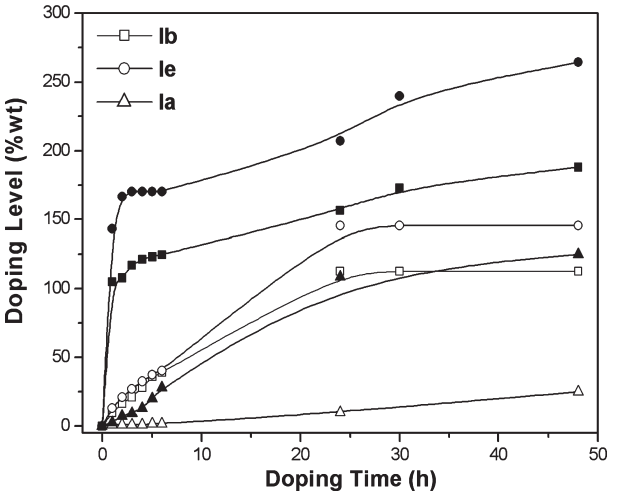

Figure 5. Time dependence of doping level (wt %) of the P[Py(x)-PrO(y)/SO_2] copolymers at 50 (open symbols) and 80 °C (closed symbols) in H_3PO_4 85%.

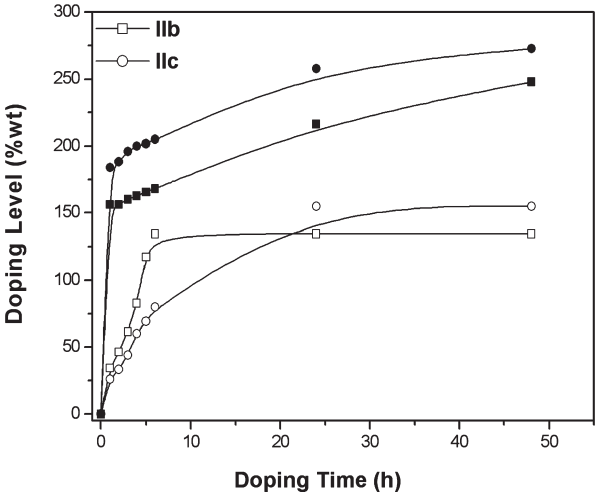

Figure 6. Time dependence of doping level (wt %) of the P[Py(x)-PrO(y)/PO] copolymers at 50 (open symbols) and 80 °C (closed symbols) in H_3PO_4 85%.

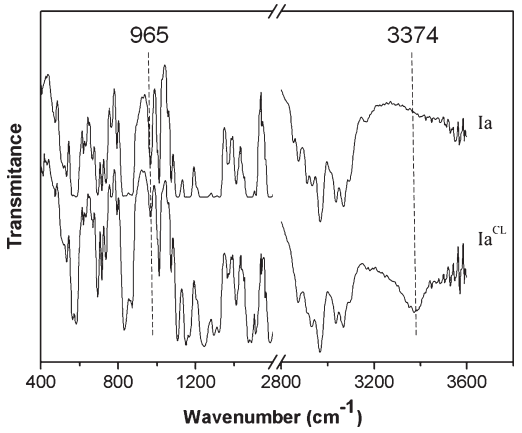

Figure 7. Comparative FT-IR spectra of the virgin polymer Ia and the cross-linked polymer $\mathbf{Ia}^{CL}$.

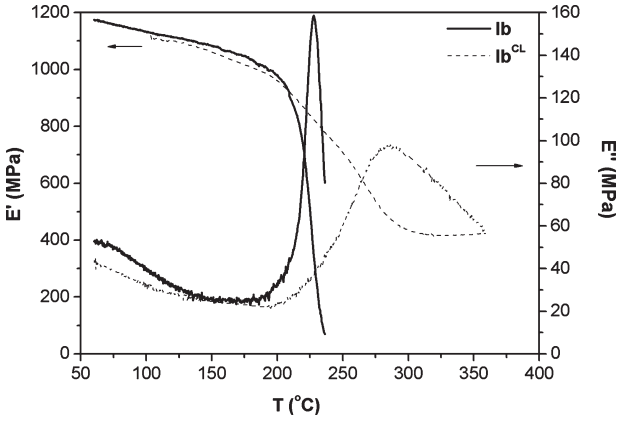

Figure 8. Comparative DMA curves of the virgin polymer **Ib** and the cross-linked polymer $\mathbf{Ib}^{CL}$.

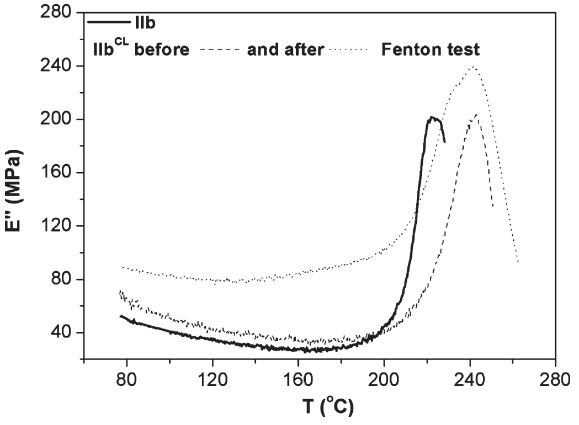

Figure 9. Comparative DMA curves of the virgin polymer **IIb** and the cross-linked polymer $\mathbf{IIb}^{CL}$ before and after treatment with H_2O_2 (Fenton test).

more phosphoric acid compared to those with the sulfone groups, although the pyridine percentage is the same. This behavior is in accordance with our previous extended research related with the influence of this group on the doping ability of various materials.[51,52] It is suggested that the phosphoric acid apart from the protonation of the pyridine ring, interacts with the phosphinoxide moieties and forms ionic clusters which lead to higher doping levels. Furthermore, it is obvious in all cases that the doping ability of all the membranes is drastically increased at elevated temperatures. This phenomenon is expected since the rise of the temperature can increase the mobility of polymer chains and the free volume for the acid adsorption, which lead to the increment of acid absorbability of the membranes.

Up to now, cross-linked polymer electrolyte membranes containing aromatic bisazides as a cross-linker have been obtained only for sulfonated polymers which are intended for use in low temperature fuel cells.[38] To the best of our knowledge the present work is the first attempt to create non-sulfonated pyridine-based cross-linked polymers using bisazide compounds for use in fuel cells with operating temperatures up to 200 °C. During the thermal treatment the bisazide loses a nitrogen and a reactive nitrene is formed. This intermediate product was added to the propenyl groups to give aziridines and amines[53,54] as shown in Scheme 2. The used amounts of the neat cross-linkable polymers and the bisazide are listed in Table 2.

The cross-linked structure was confirmed by comparing the FT-IR spectra of the virgin and the cross-linked polymers and a characteristic example is given in Figure 7 for the polymer **Ia**. The spectra are normalized at the peak of 1011 cm^{-1} which is associated with the C−O−C vibrations of the aromatic polyethers and is characteristic for both samples. The absorption peak at 965 cm^{-1} assigned to the C═C double bonds obviously decreased after the cross-linking procedure while a new broad band at 3374 cm^{-1} appeared only in the cross-linked polymer attributed to the N−H stretch vibration of the secondary amines (Scheme 2). It is therefore concluded that the bisazide was successfully incorporated with the propenyl groups to form the cross-linked network. Moreover, all the membranes which were produced from the virgin polymers have a solubility of about 70 wt % in DMAc when heated at 60 °C for 6 h while the successfully cross-linked membranes were almost insoluble under the same conditions as it can be seen in Table 2.

The effect of the cross-linking on the mechanical properties and the oxidative stability of the membranes was examined with DMA measurements. It is known that cross-linking enhances the mechanical properties of the membranes and therefore an increase to the T_g values for the cross-linked polymers is expected. Indeed, as it is shown in Figures 8 and 9 the glass transition temperatures of the cross-linked membranes $\mathbf{Ib}^{CL}$ and $\mathbf{IIb}^{CL}$ are increased compared to the virgin polymers. More specifically, the cross-linked polymer with the sulfone groups $\mathbf{Ib}^{CL}$, see Figure 8, presents a T_g value at 290 °C which is 62 °C higher compared to the not cross-linked membrane **Ib**. Furthermore, the storage modulus after cross-linking is not decreased after 300 °C but it reaches a plateau and this behavior is characteristic for the cross-linked networks. On the other hand, for the polymeric structure with the phosphinoxide moieties (Figure 9) the difference in T_g values between the cross-linked and not cross-linked membrane is only 22 °C showing that the cross-linking is not as effective as in the case of the previous polymer. The possible explanation for this phenomenon could be the sterical hindrance of the phosphinoxide units which limits the successful incorporation of the bisazide with the propenyl groups. The cross-linked membranes were subjected to the Fenton reagent to evaluate their oxidative stability. As it can be seen in Figure 9 the cross-linked membrane $\mathbf{IIb}^{CL}$, which was subjected to Fenton test preserves its

dx.doi.org/10.1021/ma200351z |*Macromolecules* 2011, 44, 4942–4951

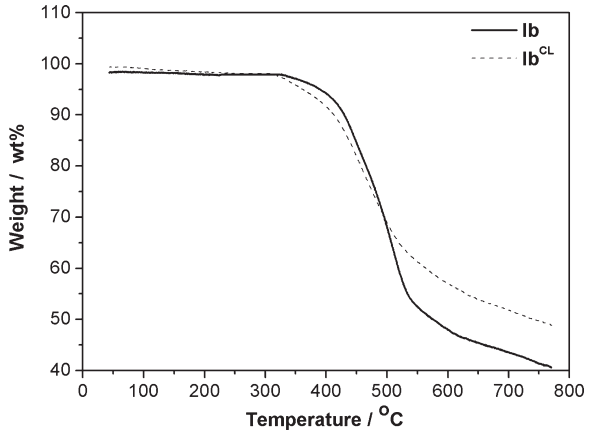

Figure 10. Comparative TGA curves of the virgin polymer **Ib** and the cross-linked polymer $\mathbf{Ib}^{CL}$.

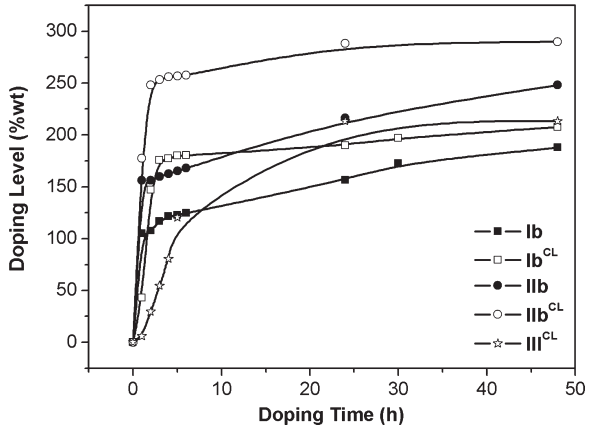

Figure 11. Comparison of the doping ability with H_3PO_4 85% at 80 °C, between the virgin polymers **Ib**, **IIb** with the cross-linked ones $\mathbf{Ib}^{CL}$, $\mathbf{IIb}^{CL}$, and $\mathbf{III}^{CL}$.

mechanical properties demonstrated thus the high oxidative stability of the cross-linked structure.

The thermal stability of the cross-linked polymers was evaluated by means of thermogravimetric analysis and a characteristic example is given in Figure 10 for the membranes **Ib** and $\mathbf{Ib}^{CL}$. The virgin polymer is thermally stable until 330 °C while for the cross-linked one, a small weight loss is observed at this temperature. As it was mentioned during the thermal treatment the bisazide mainly reacts with the propenyl groups to form the cross-linked network. However, a reaction between the intermediate reactive nitrenes is possible.[55] Hence, the small weigh loss which is observed for all the cross-linked membranes at temperatures between 330 and 500 °C compared to the azide-free membranes is probably attributed to the decomposition of these side products, while above 500 °C the superior thermal stability of the cross-linked sample is obvious. In addition, the thermal stability of the cross-linked structure is retained after the treatment with the Fenton reagent which further confirms these materials' oxidative stability.

The doping ability of the cross-linked membranes in phosphoric acid at 80 °C is depicted in Figure 11 and for comparison reasons the doping level of the virgin polymers is also presented. In general, it is known that the cross-linking leads to more

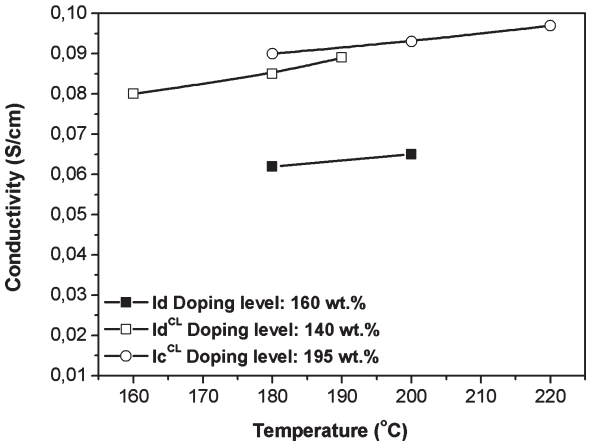

Figure 12. Temperature dependence of ionic conductivity for the **Id**, $\mathbf{Id}^{CL}$, and $\mathbf{Ic}^{CL}$ based MEAs at various doping levels. Membrane thicknesses: 140, 120, and 110 μm, respectively.

Table 3. Doping Level, Ionic Conductivity, and Current Density at 500 mV for the Id, $\mathbf{Id}^{CL}$, and $\mathbf{Ic}^{CL}$ based MEAs at 180 °C

cross-linked polymer	doping level (wt %)	ionic conductivity (S/cm)	current density at 500 mV, A/cm^2
Id	160	0.062	0.42
$\mathbf{Id}^{CL}$	140	0.088	0.61
$\mathbf{Ic}^{CL}$	195	0.09	0.72

compact chemical structures which decrease the materials' doping ability as well as its conductivity. Contrary to this, the cross-linked membranes in this work showed higher doping levels compared to the neat polymers. The explanation for this fact is the formation of the aziridines or amines functionalities which also interact with the phosphoric acid resulting thus in higher doping levels. To confirm this suggestion, a cross-linkable homopolymer P[Pro(100)/SO_2] with no polar groups was synthesized. The homopolymer was cross-linked with the bisazide as in all other cases. The acid uptake of the cross-linked homopolymer was about 200 wt % (Figure 11) under the same doping conditions while the noncross-linked polymer showed negligible doping ability. This result proves that the aziridines and the amines which are present only in the cross-linked membranes contribute to the membranes' doping ability.

In order to evaluate the effect of cross-linking on the conductivity, doped membranes have been measured in situ in a single cell reactor by means of AC impedance spectroscopy. In Figure 12 is depicted the temperature dependence of the ionic conductivity for the MEAs which were produced from the cross-linked membranes, $\mathbf{Ic}^{CL}$, $\mathbf{Id}^{CL}$, and the azide-free polymer **Id**. In general, higher doping levels lead to higher ionic conductivities (Table 3) as expected for all acid doped systems. In addition, it can be observed in all cases that the temperature increase improves the ionic conductivity. This is reasonable since at elevating temperatures the mobility of the polymeric chain increases and this enhances the proton's mobility. Furthermore, it must be noticed that although the membranes **Ic** and $\mathbf{Ic}^{CL}$ absorbed almost the same quantity of acid, the conductivity of the cross-linked membrane is slightly higher compared to the neat polymer. This fact is in agreement with previous studies by our

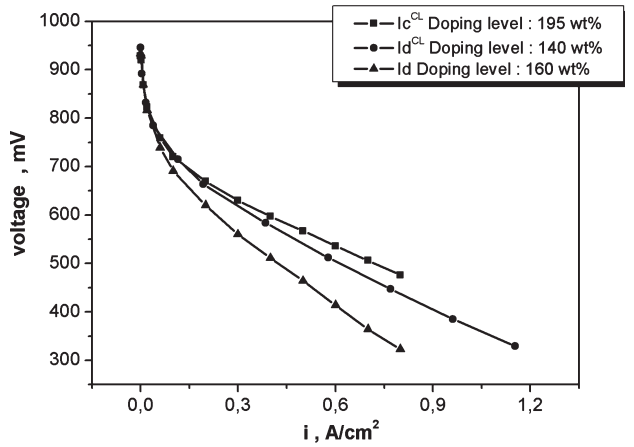

Figure 13. Current- voltage curves for the **Id**, **Id**^{CL}, and **Ic**^{CL} based MEAs at various doping levels at 180 °C using dry gases with anode (H_2) and cathode (air) stoichiometric ratio of 1.2 and 2, respectively, at ambient pressure with an active area of 25 cm^2 .

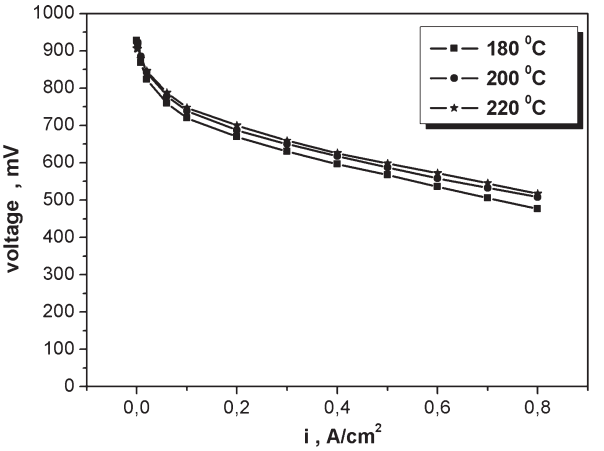

Figure 14. Current−voltage curves for the cross-linked copolymer **Ic**^{CL} at several operating temperatures between 180 and 220 °C using dry gases with anode (H_2) and cathode (air) stoichiometric ratio of 1.2 and 2, respectively, at ambient pressure. Conditions: doping level, 195 wt %; membrane thickness, 120 μm; active area, 25 cm^2.

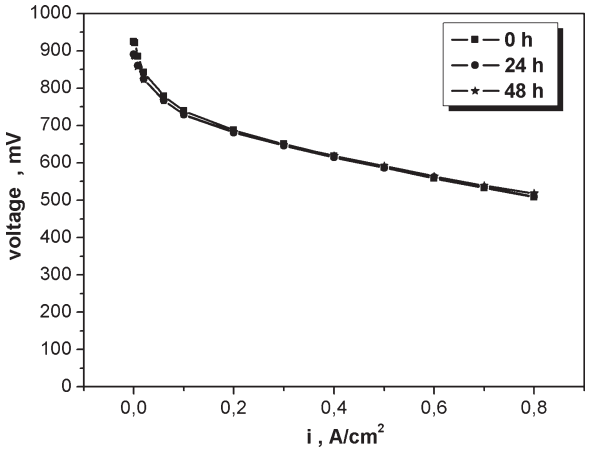

Figure 15. Current−voltage curves of MEA based on the cross-linked copolymer **Ic**^{CL} during 48 h at 200 °C using dry gases with anode (H_2) and cathode (air) stoichiometric ratio of 1.2 and 2, respectively, at ambient pressure. Conditions: doping level, 195 wt %; membrane thickness, 120 μm; active area, 25 cm^2.

research group, related to the effect of the polymeric structure on the conductivity.[56,57] According to these results not only the doping level but the whole polymeric matrix affects the final ionic conductivity of the polymers. More specifically, in the cross-linked structure the presence of the aziridines or amines not only increases the materials doping ability but the conductivity as well. It should be mentioned that although the cross-linking is known to decrease the ionic conductivity,[58−60] in our case the selected cross-linker created functional groups which provided more pathways for the proton transfer and subsequently higher conductivity values were noticed.

Selected cross-linked membranes were used for membrane electrode assembly preparation as exemplified in the Experimental Section and these MEAs were tested in a single cell. In Figure 13 are depicted the current−voltage (polarization) curves at 180 °C for the MEAs which were produced from the cross-linked membranes, **Ic**^{CL}, **Id**^{CL} and the azide free membrane **Id**. These curves imply that the fuel cell performance of MEAs based on the cross-linked copolymers (**Ic**^{CL} and **Id**^{CL}) was improved compared to the neat copolymer **Id**. As shown in Table 3 the improvement of the performance of MEA based on the cross-linked copolymer **Id**^{CL} is remarkable and in particular the current density at cell voltage of 0.5 V is 0.61 A/cm^2 and this value is almost 50% higher compared to the virgin copolymer. Furthermore, the performance of the MEA based on the cross-linked copolymer **Ic**^{CL} is better compared to the **Id**^{CL} based MEA. This is reasonable since higher doping levels lead to higher ionic conductivities as already has been mentioned. Figure 14 illustrates the polarization curves for the MEA based on the cross-linked copolymer **Ic**^{CL} at several operating temperatures between 180 and 220 °C using dry gases with anode (H_2) and cathode (air) stoichiometric ratio of 1.2 and 2, respectively, at ambient pressure. These curves indicate that the fuel cell performance was improved with increasing temperatures from 180 to 220 °C, which can be easily explained by the increase of the membrane's conductivity at higher temperatures. The maximum performance is observed at 220 °C with a current density of 0.83 A/cm^2 at cell voltage of 0.5 V. At this point it is worth mentioning that the cross-linking of acid doped membranes can further increase the long-term operation of the MEAs since it prevents the creep of the doped membranes. This phenomenon is often considered as the main reason for the declined performance during the fuel cell operation.[61] Hence, in order to study the stability of the fuel cell operation at 200 °C, the MEA based on the cross-linked copolymer **Ic**^{CL} was left to operate at this temperature for 48 h. The results are depicted in Figure 15, and it is obvious that the performance of the MEA is stable. To the best of our knowledge this is the first time that a cross-linked polymer for use in PEMFCs is operated at such high temperatures. However, the stability of the fuel cell performance has to be studied for longer time and research to this direction is currently in progress.

4. CONCLUSIONS

High molecular weight cross-linkable polymers were successfully synthesized by introducing propenyl groups onto pyridine based aromatic polyethers and characterized with regard to their oxidative stability and their thermal and mechanical properties as well as their ability to absorb phosphoric acid. These polymers

were subjected to thermal cross-linking using a bisazide as a cross-linker and the effect of the cross-linking on the properties of the membranes were studied. The increased T_g values for the cross-linked polymers compared to the azide-free membranes indicates that the azide-assisted cross-linking has successfully improved the mechanical properties of the membranes. Moreover, the cross-linking modification played an important role in improving the doping ability and the conductivity of the resulted cross-linked membranes compared to their virgin analogues. The preparation of MEAs and the preliminary fuel cell tests showed that the cross-linked materials present superior performances compared to the neat polymers. Moreover, the operation of the cross-linked membranes at temperatures higher than 200 °C in combination with the stable performance at 200 °C for 48 h demonstrate the feasibility of these type of electrolytes to be used in high temperature PEM fuel cells.

AUTHOR INFORMATION

Corresponding Author

*Telephone: (+30)2610-962952. Fax: (+30)2610-997122. E-mail: j.kallitsis@upatras.gr.

ACKNOWLEDGMENT

Financial support of this work from the European Commission through the programs "Development of an Internal Reforming Alcohol High Temperature PEM Fuel Cell Stack", IRAFC FCH-JU 245202 (2010−2012), and "Understanding the Degradation Mechanisms of Membrane-Electrode-Assembly for High Temperature PEMFCs and Optimization of the Individual Components", DEMMEA FCH-JU 245156 (2010-2012), is greatly acknowledged.

REFERENCES

(1) Steele, B. C. H.; Heinzel, A. *Nature* **2001**, *414*, 345–352.
(2) Rikukawa, K.; Sanui, M. *Prog. Polym. Sci.* **2000**, *25*, 1463–1502.
(3) Hickner, M. A.; Ghassemi, H.; Kim, Y. S.; Einsla, B. R.; McGrath, J. E. *Chem. Rev.* **2004**, *104*, 4587–4612.
(4) Li, Q. F.; He, R. H.; Jensen, J. O.; Bjerrum, N. J. *Chem. Mater.* **2003**, *15*, 4896–4915.
(5) Kreuer, K. D. *J. Membr. Sci.* **2001**, *185*, 29–39.
(6) Mauritz, K. A.; Moore, R. B. *Chem. Rev.* **2004**, *104*, 4535–4585.
(7) Wang, Y.; Chen, K. S.; Mishler, J.; Cho, S. C.; Adroher, X. C. *Appl. Energy* **2010**, *88*, 981–1007.
(8) Lee, J. K.; Kerres, J. *J. Membr. Sci.* **2007**, *294*, 75–83.
(9) Kim, H. J.; Krishnan, N. N.; Lee, S. Y.; Hwang, S. Y.; Kim, D.; Jeong, K. J.; Lee, J. K.; Cho, E.; Lee, J.; Han, J.; Ha, H. Y.; Lim, T. H. *J Power Sources* **2006**, *160*, 353–358.
(10) Chen, K.; Chen, X.; Yaguchi, K.; Endo, N.; Higa, M.; Okamoto, K. *Polymer* **2009**, *50*, 510–518.
(11) Wang, F.; Hickner, M.; Kim, Y. S.; Zawodzinski, T. A.; McGrath, J. E. *J. Membr. Sci.* **2002**, *197*, 231–242.
(12) Einsla, B. R.; Kim, Y. S.; Hickner, M. A.; Hong, Y. T.; Hill, M. L.; Pivovar, B. S.; McGrath, J. E. *J. Membr. Sci.* **2005**, *255*, 141–148.
(13) Wang, F.; Hickner, M.; Ji, Q.; Harison, W.; Mecham, J.; Zawodinski, T. A.; McGrath, J. E. *Macromol. Symp.* **2001**, *175*, 387–396.
(14) Lee, C. H.; Park, H. B.; Chung, Y. S.; Lee, Y. M.; Freeman, B. D. *Macromolecules* **2006**, *39*, 755–764.
(15) Li, X. F.; Chen, D. J.; Xu, D.; Zhao, C. J.; Wang, Z.; Lu, H.; Na, H. *J. Membr. Sci.* **2006**, *275*, 134–140.
(16) Yin, Y.; Hayashi, S.; Yamada, O.; Kita, H.; Okamoto, K. *Macromol. Rapid Commun.* **2005**, *26*, 696–700.
(17) Zhong, S.; Cui, X.; Cai, H.; Fu, T.; Shao, K.; Na, H. *J. Power Sources* **2007**, *168*, 154–161.
(18) Hofmann, M. A.; Ambler, C. M.; Maher, A. E.; Chalkova, E.; Zhou, X. Y.; Lvov, S. N.; Allcock, H. R. *Macromolecules* **2002**, *35*, 6490–6493.
(19) Kerres, J.; Ullrich, A.; Meier, F.; Häring, T. *Solid State Ionics* **1999**, *125*, 243–249.
(20) Kerres, J. A. *Fuel Cells* **2005**, *5*, 230–247.
(21) Deimede, V.; Voyiatzis, G. A.; Kallitsis, J. K.; Qingfeng, L.; Bjerrum, N. J. *Macromolecules* **2000**, *33*, 7609–7617.
(22) Feng, S.; Shang, Y.; Wang, S.; Xie, X.; Wang, Y.; Wang, Y.; Xu, J. *J. Membr. Sci.* **2010**, *346*, 105–112.
(23) Thomas, O. D.; Peckhan, T. J.; Thanganathan, U.; Yang, Y.; Holdcroft, S. *J. Polym. Sci., Part A: Polym. Chem.* **2010**, *48*, 3640–3650.
(24) Li, Q.; Pan, C.; Jensen, J. O.; Noyé, P.; Bjerrum, N. J. *Chem. Mater.* **2007**, *19*, 350–352.
(25) Zhang, W.; Gogel, V.; Friedrich, K. A.; Kerres, J. *J. Power Sources* **2006**, *155*, 3–12.
(26) Wainright, J. S.; Wang, J. T.; Weng, D.; Savinell, R. F.; Litt, M. *J. Electrochem. Soc.* **1995**, *142*, L121–L123.
(27) Ma, Y. L.; Wainright, J. S.; Litt, M.; Savinell, R. F. *J. Electrochem. Soc.* **2004**, *151*, A8–A16.
(28) Carollo, A.; Quartarone, E.; Tomasi, C.; Mustarelli, P.; Belotti, F.; Magistris, A.; Maestroni, F.; Parachini, M.; Garlaschelli, L.; Righetti, P. P. *J. Power Sources* **2006**, *160*, 175–180.
(29) Li, Q.; Jensen, J. O.; Savinell, R. F.; Bjerrum, N. *J. Progr. Polym. Sci.* **2009**, *34*, 449–477.
(30) Gourdoupi, N.; Andreopoulou, A. K.; Deimede, V.; Kallitsis, J. K. *Chem. Mater.* **2003**, *15*, 5044–5050.
(31) Pefkianakis, E. K.; Deimede, V.; Daletou, M. K.; Gourdoupi, N.; Kallitsis, J. K. *Macromol. Rapid Commun.* **2005**, *26*, 1724–1728.
(32) Gourdoupi, N.; Kallitsis, J. K.; Neophytides, S. G. *J. Power Sources* **2010**, *195*, 170–174.
(33) Kallitsis, J. K.; Geormezi, M.; Neophytides, S. G. *Polym. Int.* **2009**, *58*, 1226–1233.
(34) Zhong, S.; Cui, X.; Cai, H.; Fu, T.; Zhao, C.; Na, H. *J. Power Sources* **2007**, *164*, 65–72.
(35) Ding, F. C.; Wang, S. J.; Xiao, M.; Meng, Y. Z. *J. Power Sources* **2007**, *164*, 488–495.
(36) Zhong, S.; Cui, X.; Cai, H.; Fu, T.; Shao, K.; Na, H. *J. Power Sources* **2007**, *168*, 154–161.
(37) Ding, F. C.; Wang, S. J.; Xiao, M.; Li, X. H.; Meng, Y. Z. *J. Power Sources* **2007**, *170*, 20–27.
(38) Oh, Y. S.; Lee, H. J.; Yoo, M.; Kim, H. J.; Han, J.; Kim, K.; Hong, J. D.; Kim, T. H. *Chem. Commun.* **2008**, 309–315.
(39) Feng, S.; Shang, Y.; Xie, X.; Wang, Y.; Xu, J. *J. Membr. Sci.* **2009**, *335*, 13–20.
(40) Zhong, S.; Liu, C.; Na, H. *J. Membr. Sci.* **2009**, *326*, 400–407.
(41) Zhou, S.; Kim, J.; Kim, D. J. *Membr. Sci.* **2010**, *348*, 319–325.
(42) Lee, K. S.; Jeong, M. H.; Lee, J. P.; Lee, J. S. *Macromolecules* **2009**, *42*, 584–590.
(43) Jeong, M. H.; Lee, K. S.; Lee, J. S. *Macromolecules* **2009**, *42*, 1652–1658.
(44) Jeong, M. H.; Lee, K. S.; Lee, J. S. *J. Membr. Sci.* **2009**, *337*, 145–152.
(45) Lee, K. S.; Jeong, M. H.; Lee, J. S.; Pivovar, B. S.; Kim, Y. S. *J. Membr. Sci.* **2010**, *352*, 180–188.
(46) Smith, C. D.; Gungor, A.; Keister, K. M.; Marand, H. A.; McGrath, J. E. *Polym Prepr (Am Chem Soc Div Polym Chem)* **1991**, *32*, 93–95.
(47) Price, C.; Snyder, W. *J. Am. Chem. Soc.* **1961**, *83*, 1773.
(48) Shang, X. Y.; Li, X. H.; Xiao, M.; Meng, Y. Z. *Polymer* **2006**, *47*, 3807–3813.
(49) Hubner, G.; Roduner, E. J. *J. Mater. Chem.* **1999**, *9*, 409–418.
(50) Cosmala, B.; Schauer, J. *J. Appl. Polym. Sci.* **2002**, *85*, 1118–1127.
(51) Gourdoupi, N.; Papadimitriou, K.; Neophytides, S.; Kallitsis, J. K. *Fuel Cells* **2008**, *8*, 200–208.

(52) Daletou, M. K.; Geormezi, M.; Pefkianakis, E. K.; Morfopoulou, C.; Kallitsis, J. K. *Fuel Cells* **2010**, *10*, 35–44.
(53) Jia, J.; Baker, G. L. *J. Polym. Sci., Part B: Polym. Phys.* **1998**, *36*, 959–968.
(54) Roy, D.; Basu, P. K.; Raghunathan, P.; Eswaran, S. V. *Magn. Reson. Chem.* **2003**, *41*, 671–678.
(55) Yasuda, N.; Yamamoto, S.; Wada, Y.; Yanagida, S. *J. Polym. Sci., Part A: Polym. Chem.* **2001**, *39*, 4196–4205.
(56) Geormezi, M.; Deimede, V.; Gourdoupi, N.; Triantafyllopoulos, N.; Neophytides, S.; Kallitsis, J. K. *Macromolecules* **2008**, *41*, 9051–9056.
(57) Daletou, M. K.; Kallitsis, J. K.; Voyiatzis, G.; Neophytides, S. G. *J. Membr. Sci.* **2009**, *326*, 76–83.
(58) Kerres, J.; Cui, W.; Disson, R.; Neubrand, W. *J. Membr. Sci.* **1998**, *139*, 211–225.
(59) Zhang, C.; Guo, X.; Fang, J.; Xu, H.; Yuan, M.; Chen, B. *J. Power Sources* **2007**, *170*, 42–45.
(60) Mikhailenko, S. D.; Wang, K.; Kaliaguine, S.; Xing, P. *J. Membr. Sci.* **2004**, *233*, 93–99.
(61) Mader, J. A.; Benicewicz, B. C. *Macromolecules* **2010**, *43*, 6706–6715.